

# Melt Flow and Dopant Distribution During the Growth of Si and Ge Crystal: A Review

Tinghui Zhang\*, Ansheng Zheng, Jialiang Zhang

General Research Institute for Nonferrous Metals, Beijing 100088, China  
 ZhangThui110@163.com

Segregation occurs for most of dopants employed in crystal growth, leading to variation of dopant concentration and properties along the crystal. This article presented a review of recent research on melt flow and dopant distribution during the growth of Si and Ge crystal. The effects of melt flow and segregation on the dopant distribution in systems including Czochralski indium doped germanium crystals, Czochralski B-Ge codoped silicon crystals, and Ga doped germanium crystals grown by the VB method. The convection, solute distribution, and their effect on resistivity distribution during CZ antimony doped germanium single crystal still need further investigation.

## 1. Introduction

In crystal growth, impurities are generally added to the melt to obtain desired dopant concentration and therefore desired properties (Cartalade et al., 2016). Segregation occurs for most of dopants employed in the growth of Germanium and Silicon crystal growth, leading to spatial variation of dopant concentration and consequently electrical and optical properties (Sabanskis et al., 2015.). In order to grow crystals with uniform axial and radial resistivity distribution, it is essential to control the segregation (Aghamaliyev et al., 2016; Khlybov and Lyubimova, 2016; Nawaz et al., 2015). Concentration profile of dopants in crystal grown under equilibrium condition could be described by normal freezing equation:  $C = k_0 C_0 (1-g)^{k-1}$ .

Where  $C_0$  is the initial solute concentration in the melt before the solidification,  $g$  is the solidification fraction,  $C$  is concentration in crystal and  $k_0$  is the equilibrium segregation coefficient (Podkopaev et al., 2016.). The equilibrium segregation coefficient was defined as the ratio of dopant concentration in the solid and melt under equilibrium condition, where the solidification rate is extremely slow, and there is thus sufficient time to reach uniform distribution of dopants through diffusion in both solid and liquid phase (Cristiano et al., 2016).

In practical crystal growth process, however, it is hardly possible to reach the equilibrium condition, taking into account the productive efficiency. Therefore, the normal solidification equation is not sufficient to predict the concentration profile in crystal.

For dopants with  $k_0 < 1$ , the impurity atoms are consistently rejected to the melt near the solid-liquid interface, leading to rise of dopant concentration. If these accumulating dopant atoms could not be taken away through diffusion and convection, a concentration sublayer would form, which is bad for concentration and resistivity uniformity along the grown crystal.

A series of numerical simulations and experimental research emerged in order to describe the concentration and resistivity distribution along crystal. There are mainly two ways to tackle this problem. One way is to use effective segregation coefficient instead of equilibrium segregation coefficient to predict the dopant distribution. The other is to investigate the melt flow behavior to analyze the solute concentration near the interface, which is used then to calculate the dopant distribution in the crystal.

First of all, we introduce the background of this study. Reflective high energy electron diffraction is based on the diffraction effect of the periodic structure of the crystal on high-energy electrons to determine the surface and internal structure of the crystal. As the representative of the third generation semiconductor materials, Si C has the advantages of wide band gap, high thermal conductivity and high saturation electron drift rate relative to common Si and Ga As semiconductor materials. In the monitoring process of crystal growth, the interpretation of RHEED pattern can effectively determine the state of crystal growth and the pattern of growth.

Unlike low energy electron diffraction, the electron beam is grazing incidence in the RHEED system and does not affect the growth of the material at the same time. So it is widely used in the material growth system such as MBE, CVD and other materials to monitor the material growth in real time.

At present, the doping of SiC is mainly focused on the work of N type impurities (nitrogen, phosphorus, etc.) and P type impurities (boron, aluminum and so on), but less study of the influence of the doping of the IV impurity elements (germanium, tin and so on) on the SiC crystal material. The growth of germanium islands on silicon substrates by self-assembly effect has attracted wide attention in the past more than 10 years. Since the presence of Ge elements can reduce the contact resistance of electronic devices and increase the electron mobility and life, the current gain in the heterostructure tube (HBT) with Ge silicon carbide substrate is increased by 50%, and the initial voltage increases by 33%. At the same time, because of the compatibility with the traditional silicon technology, the Si Ge heterostructure epitaxy has a broad application space, and the monitoring technology of its growth is particularly important.

In this paper, based on the basic crystal diffraction theory, the RHEED patterns in different process conditions and different growth stages are interpreted in order to determine the pattern and state of crystal growth. By adjusting the doping amount of Ge to regulate the lattice parameters and band structure of SiC materials, the application of SiC materials in the energy band engineering can be better played, so that the SiC devices have more structure to choose, and the performance of the devices will be greatly improved. In 2015, the theoretical simulation results of Ghosh and so on showed that when the doping amount of Ge in 3C-SiC reached 10.59wt%, the structure of SiC crystal changed and the band structure changed, from the original indirect band gap to direct band gap semiconductor. The analysis of diffraction patterns of different growth stages and patterns is given. The relationship between the RHEED pattern and the internal structure of the crystal is established, and the corresponding technological conditions for the evolution of the diffraction pattern are given.

## 2. Effective segregation coefficients and solute sublayer

A thermodynamic based theory was first established by Thurmond and Struther to calculate the segregation coefficients of certain impurities. proposed a modified theory taking into account the lattice distortion energy and the formation energy of the vacancies to calculate the segregation coefficients of a series of solute in silicon and germanium. It shows that the segregation coefficients of solute such as tin (Sn), lead (Pb), arsenic (As), and indium (In) agree well with experimental result, while the predicted segregation coefficient of Ga (Ga) and Antimony (Sb) had large discrepancy with experimental results.

Calculated the segregation coefficient of Ga in Ga-B co-doped silicon crystals based on thermodynamic theory by taking into account the distortion energy of impurity atoms in crystal lattice. Then the normal solidification equation was applied to fit the experimental data to yield the effective coefficient, which was compared with the calculated value. It shows that co-doping with B suppressed the segregation of Ga in Ge. The dopant concentration in this study was transformed from converting the measured resistivity values.

To investigate the relation between concentration distribution of in CZ-Germanium crystal and its electrical properties, conducted a low-temperature Hall effect measurement on samples taken from different axial and radial positions. The dopant concentration was calculated and then fitted by normal freezing equation, obtaining the effective segregation coefficient.

Studied the segregation of germanium in B-Ge co-doped silicon crystals. The solute concentration was measured using electron probe microanalysis (EPMA), and the effective segregation coefficient was calculated using the same fitting method as Xinming Huang and Guojian Wang. The effect of initial solute concentration in the melt on segregation was investigated.

Used directional solidification methods with immersed heater to grow Ga doped Germanium crystals, and explored the effect of external stirring on solute concentration distribution. The resistivity of the sample was measured using a four-probe method, which was then transformed to solute concentration and fitted by Tiller's equation to get the thickness  $\delta$  of the solute concentration transient region.

Established a self-consistent solidification model to fit the experimental data of gallium-doped and antimony-doped single crystals. The effective segregation coefficient and the diffusion coefficient of the solute in liquid phase was calculated. The segregation data proposed by Burton et al. was also reinterpreted.

The physical gas phase transmission (PVT) is used to grow Ge doped and non doped silicon carbide crystals. The growth system mainly includes the medium frequency induction heating system, the vacuum system, the growth system and the cooling system of graphite materials. The equipment used for material growth is a home-made MBE system, consisting of three chambers with different vacuum standards, a sampling chamber, a preconditioning room and a growth room (the limit vacuum of the growth room can reach  $10^{-8}$  Pa). When Ge doped crystals are grown. The metal Ge powder is used as dopant, and the dopant is mixed with SiC polycrystalline powder evenly and placed at the bottom of the crucible. The growth of silicon and germanium is

evaporated by electron gun and Knudson source furnace respectively. The sample and beam sources are controlled accurately by thermocouple, shown as Figure 1.

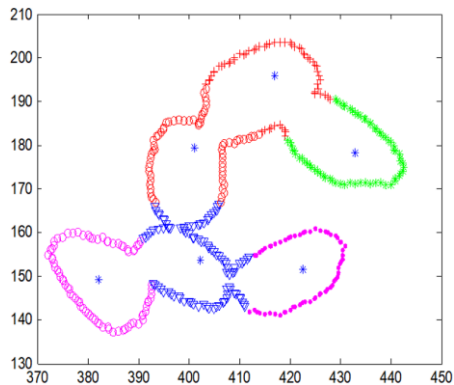


Figure 1: is the result of edge information clustering

The silicon wafer (2 inches) was first treated by standard RCA chemical cleaning process and then placed in a vacuum chamber. After 30 min heating at 500 C, the adsorbed gas was removed, and then the growth chamber was introduced into the cell. The surface passivation layer was removed at 1000 degree annealing in an ultra high vacuum environment. The grown doping and non doped crystals are cut along the vertical plane respectively. Each crystal can get 1 central longitudinal sections and 6 semicircle 2 inch cross sections. After standard grinding and polishing, the samples can be obtained. The growth rate of silicon is controlled by the current and accelerated voltage of the electron gun when the silicon buffer layer is sometimes grown on the surface of the substrate (several hundred nanometers to several microns) on the substrate before the growth of germanium.

### 3. Melt flow and mass transport

Conducted a 2D-3D coupled simulation on the melt convection mode during the growth process of Czochralski crystals. Thermal data is calculated by commercial software CrysMAS, and the boundary conditions are extracted from it for lateral application in the flow velocity field calculation conducted in ANSYS-cfx. The convective mode before and after the application of the TMF magnetic field, and its effect on the heat transfer and cross-sectional shape of the crystal was analyzed.

Simulated the melt flow in the VB growth of the doping crystal VB method and analyzed the effect of thermal diffusion and convection (represented by Soret coefficient  $\sigma$  and Grashof number  $Gr$ , respectively) on the distribution of solute in the crystal and melt. The solute concentration in the crystal at any instant was calculated using the solute concentration in the melt near the growth interface obtaining solute profile along entire crystal and melt. The results show that the effect of segregation could be suppressed by negative thermal diffusivity ( $\sigma < 0$ ) and strong convection strength ( $Gr$ ).

Employed the PANS model to solve the melt flow problem in Czochralski crystal growth, and calculated the flow characteristic parameters and convection structure. The influence of different PANS filter parameters on the calculation accuracy was evaluated. The software used is ANSYS-FLUENT. The results show that the PANS model can accurately capture the three-dimensional flow characteristics and convection structure of the Czochralski melt.

Used the low Reynolds number model to perform global simulation of the Czochralski growth process of 100 mm silicon single crystals based on the general software FLUENT. The transmission of oxygen impurities in the furnace, temperature distribution, melt flow velocity field, turbulence effect and concentration distribution along the solid-liquid interface were analyzed. The feasibility of simulating various physical phenomena in the crystal growth process by FLUENT was proved. The computational accuracy when different turbulent model was employed was compared.

Used global numerical simulation and silicon melt solidification experiments to study the effect of stirring rate on melt flow and solute concentration, based on the properties of turbulent boundary layers. The results show that with constant crystallization rate, the effective diffusion rate increases with the stirring rate. When the effective diffusivity extended a certain threshold, the mass transport transformed from a diffusive regime to a convective regime. It shows that turbulent flow can move the over accumulated dopant atom near the crystallization front and make the axial concentration distribution of the crystal more uniform.

Established a one-dimensional model to calculate the distribution of Al and In impurities in silicon-doped single crystals. The double feeding method consistently add impurities to the melt during crystal growth, and a uniform solute concentration of silicon crystals is obtained by adjusting the feeding rate of the melt using germanium and silicon rods.

The doping concentration of SIMS can be measured by EAG's SIMS, and the sensitivity of most elements can reach ppm or even the order of magnitude. A layer of silicon dioxide protection film is formed on the surface of a silicon substrate after hydrofluoric acid treatment. It can be annealed in a vacuum system to remove the oxide layer before growth. The Bruker D8 Discover high resolution X ray diffractometer was used to test the rocking curve of the sample surface to characterize the crystal quality and the change of lattice constant. Due to the different annealing temperature, the surface of silicon substrate can be reconstructed after annealing.

The RHEED pattern produced on the Si surface is integer stripes and Laue rings. The phonon Raman spectra of different SiC crystal types are obviously different due to their different structures. Therefore, phonon Raman spectroscopy is a reliable way to identify SiC polytypes. Figure 2 shows the Raman spectra of Ge doped and non doped samples under the same conditions.

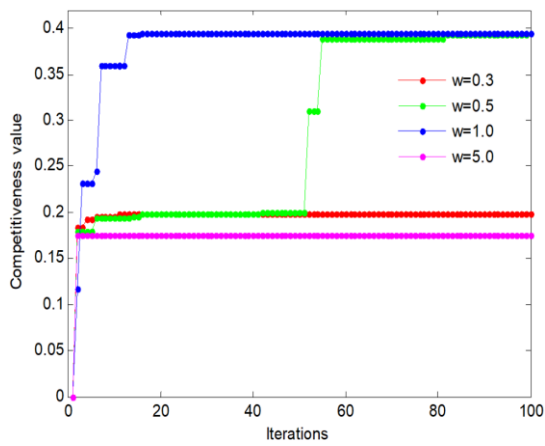


Figure 2: Changes of the optimal competitiveness of the industrial cluster along with the value of  $W$

#### 4. Transmissive diffraction patterns

Because of the difference between the lattice constants of silicon and germanium 4.2%, there is a large lattice mismatch. In the initial stage of the epitaxial growth of germanium on the silicon substrate, the epitaxial growth is in the common growth region. The germanium crystals are bound in the silicon crystal structure and accumulated a lot of stress. In the RHEED system, the high energy electron beam is incident to the surface of the crystal with a very small incident angle. Once the surface becomes an island, the electron beam will not only reflect on the crystal surface, but transmisses through the island, and the scattering beam forms on the screen to form a transmission diffraction pattern. Fig. 3. The surface corrosion morphology of Ge doped and non doped samples is observed by LEXT microscope. The dislocation density of Ge doped samples is doubled than that of non doped samples.

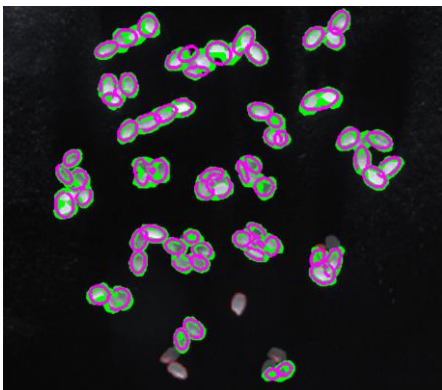


Figure 3: The complete result of segmentation

The diffraction pattern at this time will directly reflect the lattice structure inside the island, which is the distribution of lattice points in reciprocal space. The partial orientation of BPD was not revealed due to the fixed bias of the sample. In addition, due to the diffusion of electron beam energy, the corresponding Ewald sphere may not be a geometric sphere, but a spherical shell formed by a series of continuous radius spherical surfaces. As long as the inversion point in the spherical shell may be reflected on the diffraction pattern, that is, the overlapping image of the multi layer lattice points is created. When the thickness of the germanium is more than the critical thickness (about 6 atomic layers, about 1 nm), the stress in the material is released, and the germanium material begins to grow in three dimensions, and the surface is island, that is, the island growth pattern. The four image in Figure 4 is a common transmission diffraction pattern on Ge island.

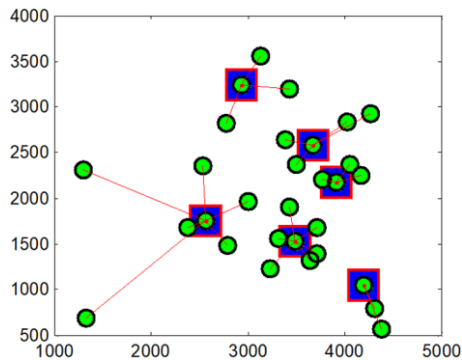


Figure 4: Stands for “the speed update+the self-adaptive variation” site selection results

## 5. Crystallization quality of Ge doped SiC crystal

In order to characterize the overall crystalline quality of Ge doped crystals and the lattice changes after doping, absolute diffraction measurements were performed using different diffraction orders on the same plane. The difference of conditions can lead to the growth of germanium amorphous or polycrystalline, especially the change of temperature is most significant. However, the diffraction of the crystal has a certain extinction condition, which is similar to that in the multi slit diffraction, and the periodic structure of the lattice can not be reflected on the diffraction pattern. The main reason for the production of BPD in Ge doped crystals is due to the large flow and floating of the group of the growth surface, which causes the nonuniform distribution of the doped elements, and the radius of the Ge atom is greater than the atomic radius of the substituted Si. First, the normals of the measured crystal surface are placed in the plane of the rays and the diffraction rays, and the diffraction tests of the doped and non doped samples are carried out (006) and (0012) surface respectively. Figure 5 Ge high resolution XRD rocking curves of (006) doped and non doped samples.

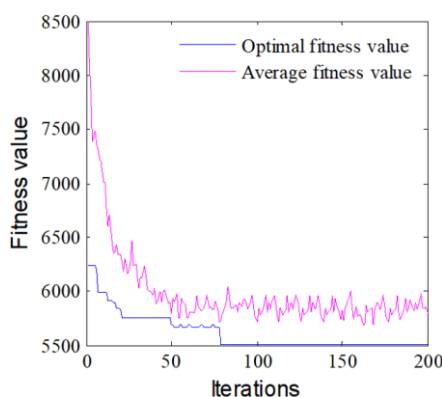


Figure 5: Stands for the standard PSO algorithm

Fig. 5 shows that the half peak width of doped samples is significantly larger than that of non doped samples, indicating that the internal defects of Ge doped crystals increase and the crystalline quality of the doped crystals decreases. It can be seen that the Prague angle of (006) plane decreases obviously, indicating that the lattice parameters of the crystal increase. In the process of material growth, the appearance of the

transmission diffraction pattern means that the surface of the material is no longer flat, the electron beam penetrates the crystal more directly instead of reflecting on the surface of the crystal, and the penetration depth in the crystal is increased.

## 6. Summary and future directions

In the crystal growth process of the Czochralski method, parameters such as crystal rotation rate, crucible rotation rate, and the height of melt free surface that continuously changes with the growth will affect the convection and mass transfer of the dopant atom, thus affecting the solute and resistivity distribution along the crystal. The effects of melt flow and segregation on the concentration distribution of solute in systems including Czochralski doped indium-gallium crystals, Czochralski boron-doped silicon crystals, and Germanium-doped crystals grown by the VB method. The convection and solute distribution during CZ antimony doped germanium single crystal and their effect on the resistivity distribution still need further investigation.

In the process of epitaxial growth of Si-Ge, RHEED is a good way to monitor crystal growth in real time. Ge doped SiC crystals were grown by PVT growth method and the defects of the crystals were studied. The doping concentration of Ge can reach  $2.52 \times 10^{18}/\text{cm}^3$ . Based on the kinematic diffraction principle of crystals, the corresponding RHEED diffraction patterns before and after SiGe crystal growth can be calculated according to the crystal structure. The mechanism of Ge doping leading to the increase of void size and dislocation at base plane was discussed. The RHEED pattern is the mapping of the crystal surface or the internal structure in the diffraction space. It can be read through the interpretation of the RHEED patterns, especially for the monitoring and analysis of the special RHEED patterns.

## References

- Aghamaliyev Z.A., Islamzade E.M., Azhdarov G.K., 2016, Modeling the distribution of Ga and Sb impurities in Ge-Si single crystals grown by double feeding of the melt: Growth conditions for homogeneous single crystals. *Crystallography Reports*, 61(2), 327-330, DOI: 10.1134/S1063774516020024.
- Cartalade A., Younsi A., Plapp M., 2016, Lattice Boltzmann simulations of 3D crystal growth: Numerical schemes for a phase-field model with anti-trapping current, *Computers & Mathematics with Applications*, 71(9), 1784-1798, DOI: 10.1016/j.camwa.2016.02.029.
- Cristiano F., Shayesteh M., Duffy R., Huet K., Mazzamuto F., Qiu Y., Quillec M., Henrichsen, H.H., Nielsen P.F., Petersen D.H., La Magna A., Caruso G., Boninelli S., 2016, Defect evolution and dopant activation in laser annealed Si and Ge. *Materials Science in Semiconductor Processing*, 42(3), 188-195, DOI: 10.1016/j.mssp.2015.09.011.
- Khlybov O.A., Lyubimova T.P., 2016, Effect of rotating magnetic field on mass transfer during directional solidification of semiconductors, *Magnetohydrodynamics*, 52(1), 61-69.
- Nawaz S.M., Dutta S., Mallik A., 2015, A comparison of random discrete dopant induced variability between Ge and Si junctionless p-FinFETs, *Applied Physics Letters*, 24(3), 1433-1440, DOI: 10.1063/1.4927279.
- Podkopaev O.I., Shimanskiy A.F., Kopytkova S.A., Filatov R.A., Golubovskaya N.O., 2016, Study of the effect of doping on the temperature stability of the optical properties of germanium single crystals, *Semiconductors*, 50(10), 1287-1290.
- Sabanskis A., Surovovs K., Virbulis J., 2015, Three-dimensional modelling of dopant transport in gas and melt during FZ silicon crystal growth, *Magnetohydrodynamics*, 51(1), 157-170.